

PII: S0017-9310(96)00286-4

Enhancement of boiling heat transfer using highly wetting liquids with pressed-on fins at low contact forces

STANLEY J. REED and ISSAM MUDAWAR†

Boiling and Two-phase Flow Laboratory, School of Mechanical Engineering, Purdue University,
West Lafayette, IN 47907, U.S.A.

(Received 13 June 1996 and in final form 9 August 1996)

Abstract—In many cooling situations, permanent attachment of fins to heat dissipating devices is undesirable yet large mechanical loads, important in reduction of thermal contact resistance, are not permitted. This work considers the interface between a low-force pressed-on fin and a heat source in boiling heat transfer; the thermal contact resistance and how the interface region may be used to promote early nucleation and gradual boiling spread. Tests were run in saturated FC-72 and FC-87 in atmospheric pressure at a range of contact pressures much lower than conventional studies and on the order of those allowable in electronic cooling. Results showed that the effect of contact pressure on contact resistance, at such low pressures, is small and that significant boiling enhancement is possible using pressed-on fins with small loads. Dissipation of up to 85 W cm^{-2} of heater surface using a non-optimized cylindrical fin at low force is demonstrated. This heat flux represents about a four-fold increase in critical heat flux (CHF) over that for a bare surface. The pressed contact fin offers the advantage of a small crevice at the fin base. Highly-wetting fluids are able to penetrate this region, superheat and nucleate earlier than with a soldered-on fin. A means of numerically modeling the boiling heat transfer from a fin is also presented. Experiments show that the nucleate boiling heat transfer coefficient is independent of the surface orientation with respect to gravity. © 1997 Elsevier Science Ltd. All right reserved.

1. INTRODUCTION

Performance of many devices, including electric motors, x-ray equipment and solid state electronics is set by the material temperature limits and the ability to handle the increasingly large heat fluxes generated. In electronic cooling, trends toward faster, more compact electronic devices and components have made traditional air cooling obsolete on large computers and foreshadowed future needs for more rigorous cooling schemes in even personal computers. Effective electronic cooling means dissipating very high heat fluxes while maintaining low, component reliability-limited, temperatures. Other aspects include ensuring the cooling device performs in a repeatable manner and minimizes temperature fluctuations.

Early liquid cooling ideas used water to cool thermally conductive devices which were attached to, or held in contact with, the heat-generating silicon components. Performance limits for such “indirect” schemes are usually set by the thermal resistance between the component and the heat sink. Directly immersing components in a coolant offers the advantage of eliminating the conduction resistances between the heat source and the coolant. Because of the intimate contact with electronic devices, however, candidate fluids for direct immersion cooling must be

highly dielectric and inert, not reacting with the component materials.

Elaborate schemes including forced convection, spray and jet impingement cooling have been demonstrated easily capable of meeting the most stringent of predicted cooling demands. In recent years, however, much attention has been given to pool boiling heat transfer as a simpler alternative. The appeal of pool boiling in electronic cooling comes from its passivity and the high heat transfer rates resulting from the vigorous, buoyancy-driven fluid flow. Without requiring the pumps and coolant lines typical of other liquid cooling schemes, pool boiling permits dissipation of a very wide range of heat fluxes with very small associated changes in temperature.

1.1. Dielectric refrigerant liquids

A family of dielectric, highly-wetting fluorocarbon compounds, with saturation temperatures at atmospheric pressure ranging from -2.25°C (L13259) to 253°C (FC-71) has been developed by 3M Company. Collectively known as “Fluorinerts”, these inert fluids have a wide range of applications including liquid chromatography, precision reflow soldering, leak and thermal shock testing for electronic components, cooling of high power devices and, because of the high solubility of oxygen and other gases in them, chemical reaction media. As a result, research involving these fluids may find use in many areas not specific to the

† Author to whom correspondence should be addressed.

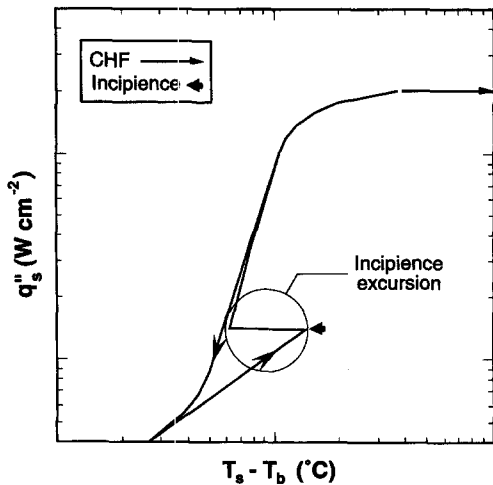


Fig. 1. Incipience excursion for a particle-blasted copper surface.

embryo size is related to both the liquid–surface contact angle and the cavity angle. For less-wetting fluids, which trap large embryos, the smallest radius is the cavity mouth radius. However, both FC-87 and FC-72 make extremely low contact angles of less than one degree with most materials. This means large surface cavities that would serve as embryo entrapment sites for less-wetting fluids are flooded and vapor embryos are only trapped in microcavities within the visible surface cavities. Because the size and geometry of these microcavities are unknown, prediction of incipience, which is often delayed to very high superheats, is difficult with the Fluorinerts. Reeber and Frieser [2] reported no nucleation even with the heater temperature 46°C higher than the fluid saturation temperature for FC-72 on a polished silicon heater surface.

When boiling finally begins, bubble growth from one cavity can extend into neighbouring ones, causing activation of those cavities. The frequent result of this is that boiling spreads rapidly over the entire surface, increasing the convection coefficient and extracting enough heat to decrease the surface temperature dramatically as shown qualitatively in Fig. 1. This decrease in temperature, known as the “incipience excursion” or “hysteresis” because the effect is only observed as heat flux is increased, constitutes a thermal shock to the electronic device which can seriously limit its life.

1.2. Surface extension and nucleation enhancement

Because both FC-87 and FC-72 have low thermal conductivities and heat capacities, the maximum pool boiling heat flux is only around 22 W cm^{-2} . This falls far below predicted future heat flux requirements for many devices and makes increased surface area necessary. Nakayama *et al.* [3] compared smooth, microfeatured, porous surfaced and multilayered porous plate fins of various lengths and reported maximum heat fluxes of up to 127 W cm^{-2} with the

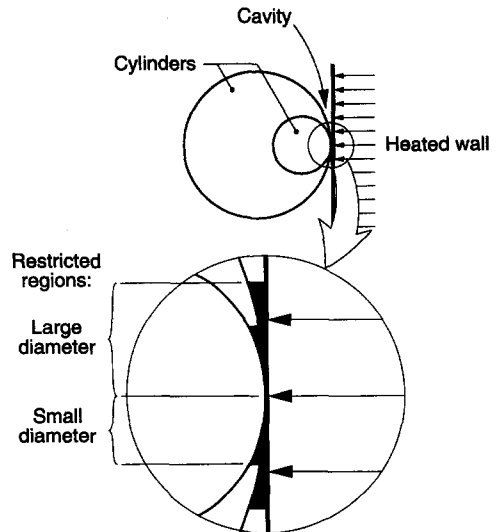


Fig. 2. Restricted regions created by interface of curved and flat surfaces (adapted from Chyu and Mghamis [6]).

multilayered porous plate fin in saturated FC-72. Anderson and Mudawar [4] examined a wide variety of fin attachments, with various surface features of different magnitudes, for both saturated and subcooled pool boiling. They reported fins capable of dissipating over 100 W for every square centimeter of base heater area for nucleate boiling in saturated liquid and up to 160 W cm^{-2} for subcooled bulk liquid. In neither investigation was the effect of contact resistance between a non-permanent attachment and the heat dissipation device considered. Furthermore, neither study considered the effect of orientation (of the boiling surface with respect to gravity) on the boiling behavior in the numerical modeling.

Permanent attachment of a fin to a heater is undesirable from assembly, maintenance and component longevity standpoints. Additionally, differences in thermal expansion coefficients of the fin and the electronic component materials can result in failure of the connection with repeated cycling, eliminating the advantage offered by the fin.

Many ideas for controlling and promoting boiling incipience at low superheats involve creation of artificial nucleation sites by surface featuring or coating with porous materials. Webb [5] summarized a variety of methods proposed for use with less-wetting fluids on heat exchanger tubes. Chyu and Mghamis [6] demonstrated that a cylinder, or any curved surface, held in contact with another surface creates a continuous array of cavities as shown in Fig. 2. Notice that, regardless of the diameter of the cylinder, the cavity angle approaches zero degrees at the point of contact and a vapor embryo will always be trapped, even with highly wetting liquids like the Fluorinerts. They found that, while all sizes of cylinders yielded lower wall superheats at incipience than that required for nucleation on a bare surface, better performance, translated as greater reduction in wall superheat,

resulting from the use of larger diameter cylinders. The effect of the cylinder, as Fig. 2 shows, is to create a "restricted region" where the natural convection-driven fluid flow is impeded. The fluid in this region is allowed to overheat, altering the temperature profile in the liquid and leading to earlier nucleation according to the Hsu and Graham [7] model for boiling incipience. Larger diameter cylinders create larger restricted regions, allowing more of the liquid to become superheated.

1.3. Study objectives

The highly-wetting Fluorinerts are capable of penetrating extremely small regions and require micro-cavities for embryo entrapment. A goal of this work is to determine whether the minute crevice at the perimeter of the interface of a heat source and a pressed-on attachment may serve as such a cavity, promoting early incipience and gradual boiling spread, eliminating the temperature overshoot associated with rapid boiling spread. Because there exist commercial products which make use of non-permanent, pressed-on attachments, extension of the concept to include boiling would be a simple matter. Unlike pure conduction devices, such as IBM's Thermal Conduction Module (TCM) described by Goth *et al.* [8] and shown in Fig. 3, manufacturing tolerances on a boiling fin could be significantly relaxed because only the flatness and uniformity of pressure between the contacting surfaces would affect the performance.

Because boiling is a complex combination of fluid flow and heat transfer processes, there is no simple solution uniformly applicable to all cooling needs. Understanding the peculiarities in the boiling behavior of the highly-wetting fluids for different cavity and surface geometries for the range of heat fluxes encountered in electronic components is critical. It is conceivable that optimal heat removal would include boiling on some interfacial geometry in addition to

surface extension. An example of a geometry optimized for heat dissipation at much greater temperatures, such as those encountered in nuclear reactor cooling, is the turnip shaped fin proposed by Cash *et al.* [9]. While the device itself is so hot that film boiling occurs on the surface, the constriction at the base of the turnip provides a temperature drop which keeps the fin in the higher heat transfer, nucleate boiling region.

For evaluation of various geometries, the thermal resistance provided by a surface attachment or fin with a boiling boundary condition must be known. Because the boiling heat transfer rate is highly temperature dependent, a simple analytical solution, as in the case of a constant convection coefficient, is not available. Applying boiling convection correlations developed for infinite, isothermal cylinders to other geometries or fins leads to considerable error. What is needed is a simple method for computing the thermal resistance of a particular fin geometry throughout natural convection and nucleate boiling in any fluid. Previous studies, including those by Anderson and Mudawar [4] and Cash *et al.* [9], have involved numerical simulation of fins using boiling boundary conditions. However, as mentioned earlier, no account was made for circumferential variation in the boiling behavior or the effect of contact resistance between the heat source and a non-permanent attachment. In this paper, a simple means of approximating the convection coefficient for use in finite difference analysis is presented.

2. EXPERIMENTAL APPARATUS AND PROCEDURE

All experiments for this study were performed in the pool boiling test chamber shown with the heater module in Fig. 4(a). The chamber consisted of a G-10 fibreglass plastic frame, top, and bottom with Lexan polycarbonate view windows on the front, back, and one side. A smaller port on the fourth side was used for adjusting the test apparatus while fluid was in the chamber. The chamber was vented to release non-condensable gases and maintain atmospheric pressure for the experiments. However, the condensing coil, with cold tap water circulated through it, recondensed nearly all the vapor, making the chamber effectively a closed system. All of the experiments were run with the same head of fluid above the submerged test heater. The 6.35 cm head corresponds to approximately 0.3°C change in, and was neglected in calculation of, the fluid saturation temperature.

Three cartridge heaters, positioned at the back of the chamber to prevent the bubbly flow from interfering with the test heater, and a cold tap water cooling coil submerged in the liquid (not shown in Fig. 4(a)), were used to maintain the bulk fluid temperature. Experiments were run with the bulk fluid subcooled 1.5°C because of the vigorous boiling-induced flow and vapor entrainment that occurred, even with a

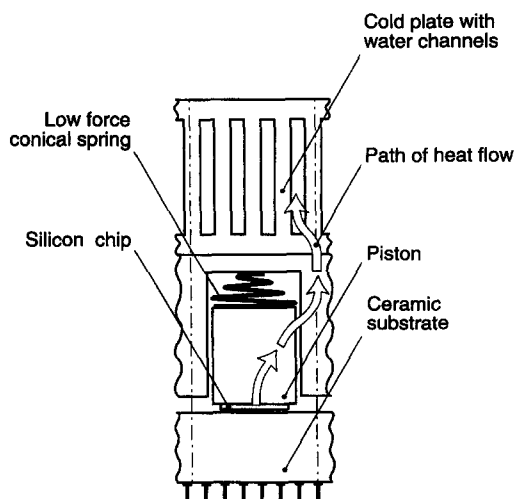


Fig. 3. Single piston section of IBM Thermal Conduction Module (adapted from Goth *et al.* [8]).

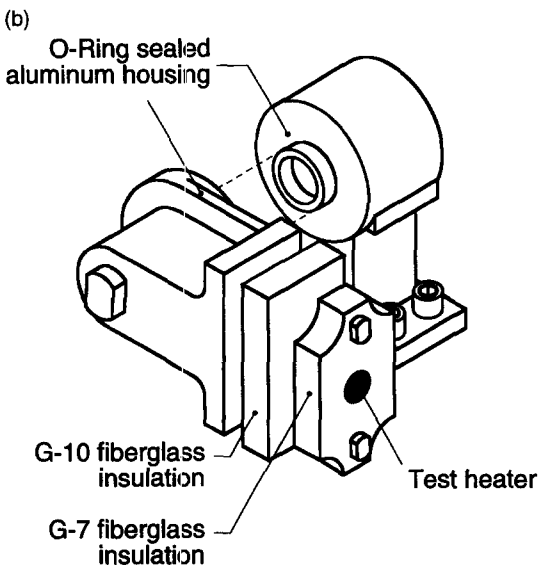
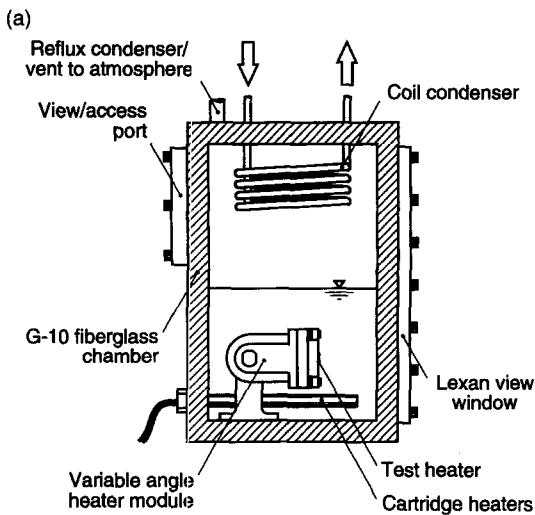


Fig. 4. (a) Test chamber; and (b) heater module.

baffle installed, when the liquid was saturated. Thermocouples mounted on an *X-Y* translation stage were positioned to measure bulk fluid temperatures in the vicinity of the test heater. Prior to each set of tests, the fluid in the chamber was vigorously boiled and recondensed for a period of thirty minutes to remove noncondensable gases.

The heater module with the test heater is shown in Fig. 4(b). The O-ring sealed module contained the heater power and thermocouple leads and could position the heater surface at any angle with respect to gravity. The test heater, detailed in Fig. 5, was made of oxygen-free copper ($k_c = 398 \text{ W m}^{-1} \text{ K}^{-1}$ at 20°C) with a 90Ω thick-film resistor soldered to the back. Electrical power provided to the resistor, measured with a power transducer and heater temperature, measured with a thermocouple 0.81 mm beneath the surface, were used to determine the surface heat flux and extrapolate the surface temperature. The heater was insulated on its perimeter and back, as shown,

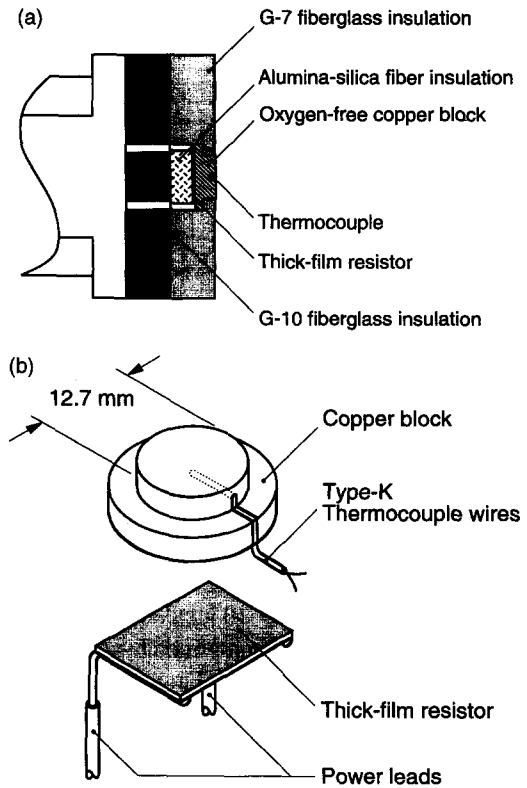


Fig. 5. (a) Heater assembly and (b) detail of test heater.

to decrease heat loss. Finite element analysis of this configuration revealed less than 2% variation in heat flux across the surface, justifying the assumptions of one-dimensional conduction through the heater and uniform heat flux across the heater surface. The heater surface temperature measurement had a maximum error at the highest heat fluxes, due to uncertainty in thermocouple position and heat flux measurement, of 5%. Although a linear calibration curve provided an excellent fit for the power transducer data, the fit had around 0.31 W offset at zero power. Inherent in very low power measurement, then, is considerable error. As a result, heat fluxes around 1 W cm^{-2} and lower are regarded with caution and those below 0.4 W cm^{-2} are excluded.

Figure 6 shows the attachment for holding fins in contact with the heater surface. The fin used in this study was an oxygen-free copper cylinder of 1.27 cm diameter and 1.6 cm length. In all tests, the fin was made adiabatic at the tip using a G-10 cylinder attached with RTV silicone sealant. A steel ball bearing at the end of the G-10 allowed the fin to self-align with the heater surface and maintained uniformity of contact pressure. A tank of compressed nitrogen was connected, through a pressure regulator, to a pneumatic actuator to provide the contact force holding the fin to the heater. The regulator was positioned outside the chamber, allowing for remote adjustment of the contact force. The force was measured using a small, 53 N load cell connected in series with the

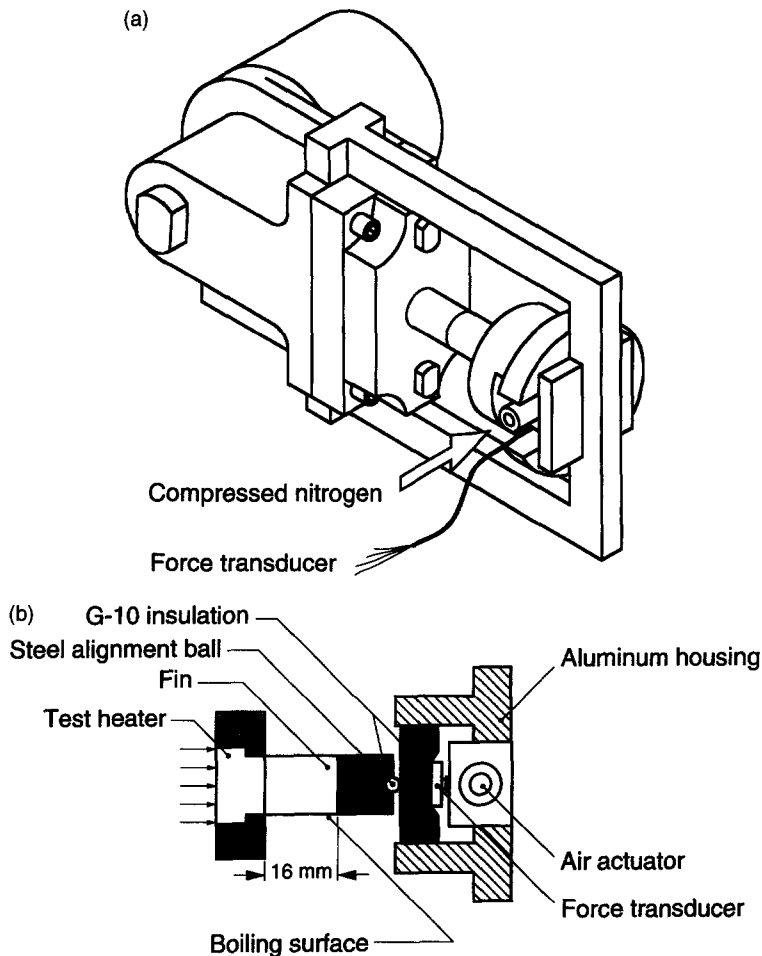


Fig. 6. (a) Heater module with surface attachment and (b) detail of extended surface attachment.

actuator. This maximum measurable force corresponded to a maximum contact pressure, for a flat-ended fin of the diameter given, of 434 kPa. This range of forces was chosen to correspond to the range of contact pressures (27–500 kPa) used by Eid and Antonetti [10] in a study of thermal contact resistances applicable to electronic components. These contact pressures are an order of magnitude smaller than those encountered in conventional contact resistance work.

Tests were run with both polished and particle-blasted mating surfaces, to determine how the roughness of the contacting surfaces affected the boiling and contact resistance behavior. In both cases, the contacting surfaces were first machined flat on a lathe and then lapped on polishing wheels using successively finer grit (to $0.05 \mu\text{m}$) to eliminate both large and small scale roughness. In the experiments where the surfaces were to be roughened, the contacting surfaces were then particle-blasted. A range of contact forces was applied and the results compared to the boiling behavior for the case of the fin soldered directly to the heater. Error in the applied force due to inaccuracy in the force transducer output and regulator adjustment varied from around 2% at the highest to nearly 20% at the lowest forces, around 2.2 N, measured.

2.1. Test procedure

Prolonged boiling and submersion in liquid has been shown to effect changes in boiling surfaces, resulting in changes in the boiling behavior. Collectively termed "surface aging", these changes were first observed by Jakob [11] and are attributed to surface oxidation, surface contamination, and continued release of gases adsorbed by the surface. To ensure uniform and repeatable boiling surface properties, the fin's boiling surface was blasted with a silica particle-water slurry (particle sizes ranged from 1 to $7 \mu\text{m}$) prior to each set of tests. Because surface aging occurs most rapidly initially, the fin surface was boiled vigorously for 30 min at one-fourth of the critical heat flux (CHF) prior to each set of tests and in conjunction with the bulk fluid deaeration, to achieve quasi-steady boiling behavior.

Power provided to the resistance heater was controlled using solid state power relays, operated by a Keithley data acquisition system (DAS), in conjunction with a resistance ladder. The data-taking was automated; the DAS monitored the heater surface and bulk fluid temperatures, heater power, and contact force, and recorded the values when the system reached steady-state. Steady-state was determined to

occur when the standard deviation of the heater temperature measurements fell below a preset limit. The system then opened or closed the power relays to increment the power. This process continued with the power relays being opened and closed, in binary-counting fashion, until critical heat flux was reached. Critical heat flux was determined to be the point when the heater temperature either did not achieve a steady value or reached 130°C, a limit set to prevent burning of the resistive heater.

3. EXPERIMENTAL RESULTS AND DISCUSSION

Because electronic components are flat, a logical location choice for a heat-dissipating device is the flat backside. It is useful, then, to evaluate the effectiveness of devices in terms of the amount of heat they can dissipate per unit heater area and the corresponding temperature of the device surface. Boiling results are presented in terms of q_s'' , the heat flux across the circular test heater surface, and $T_s - T_b$, the difference in temperature between the heater surface and the bulk fluid. For the heater-fin system, the overall thermal resistance is defined as:

$$R_t'' = \frac{T_s - T_b}{q_s''} \quad (1)$$

This resistance includes conduction through the fin, convection on the perimeter of the fin and interface region, as well as the thermal conduction contact resistance between the pressed-on fin and the heater surface. The case of the soldered-on fin is considered a limiting condition, the contact resistance is negligibly small, and the resistance made up of only conduction through the fin and convection at the surface of the fin.

3.1. Effect of mechanical pressure on contact resistance

Figure 7 summarizes results for the described copper fin held to the circular heater surface for a range of contacting forces. Tests were run using both polished, Fig. 7(a), and particle blasted, Fig. 7(b), contacting surfaces. Notice that, while the pressed-on fin behavior deviates significantly from the soldered-on, variation due to changing the contact pressure is small. Thermal contact resistance is, in general, not independent of contact pressure. When the temperature difference between mating parts is small, radiation is negligible and the heat transfer is composed of conduction through the points of true, metal-to-metal contact and conduction through the fluid that fills in the resulting gaps. The effective thickness of this fluid layer may be thought of as a mean separation distance between the parts. Even on highly polished surfaces, microscopic surface features, or asperities, cause the true area of contact to be much less than the nominal area of contact. Increased contact pressure deforms the asperities, increasing the area of true contact, and reducing the thermal contact

resistance. A decrease in the mean separation distance also accompanies the deformation, reducing the thickness of the fluid layer and its contribution to the conduction resistance. However, over the range of loads allowed on electronic components, the amount of deformation is small, making the effect of contact pressure on the contact resistance also small. Figure 7(c) compares the average polished and particle-blasted boiling behavior with boiling from a bare surface and the soldered-on fin. As expected, the rougher, particle-blasted contact shows slightly higher contact resistance, seen as a rightward shift in the boiling curve, than the polished contact.

3.2. Thermal resistance of interface

Figure 8 compares the fin resistance, determined from the soldered-on case, and the overall fin-gap resistance, using the pressed-contact with 90 kPa contact pressure. If none of the heat is lost at the interface, all of it goes through the fin and the difference between the two resistance curves, Fig. 9, gives the effective interface resistance. At low temperature differences, the natural convection heat transfer coefficient is strongly dependent on the difference in temperature. As the difference between the heater and bulk fluid temperatures approaches zero, the natural convection coefficient also goes to zero and the resistance becomes very large. Notice, from Fig. 8, that both the soldered-on and pressed-on fin resistance curves follow the expected trend for natural convection from a horizontal, isothermal cylinder given in Churchill and Chu [12] and shown qualitatively in Fig. 10(a).

Unexpectedly, the interface resistance is not constant, beginning high and dropping to a steady value of around $0.45^\circ\text{C W}^{-1}\text{ cm}^2$. This is because some heat is actually lost due to fluid circulating in the small cavities at the interface of the pressed-on fin and the heater surface. Heat removal at the interface means less of the applied heat is going through the fin, leaving the fin colder and in a region of much higher resistance at low heat fluxes. The interface resistance trend shows the value dropping below the steady resistance value (becoming negative, in some cases) between the onset of boiling and the point where boiling is occurring over the entire surface. This is because boiling began earlier, creating a greater convection coefficient, with the pressed-on fin than the soldered-on and because the pattern of boiling spread varied somewhat for successive tests. Figure 10(b) shows the dominant paths for heat flow for different heat fluxes. At low heat flux, convection at the interface, although poor, is better than the nearly infinite convection resistance offered by the cold fin. As the heat flux is increased and boiling begins, convection on the fin surface increases and dominates the interface convection, making the fin behave like the soldered-on fin and differing only, at high fluxes, by the (nearly constant) thermal contact resistance.

Boiling spread at various heat fluxes is shown for both the soldered-on and pressed-on cases in Fig. 11.

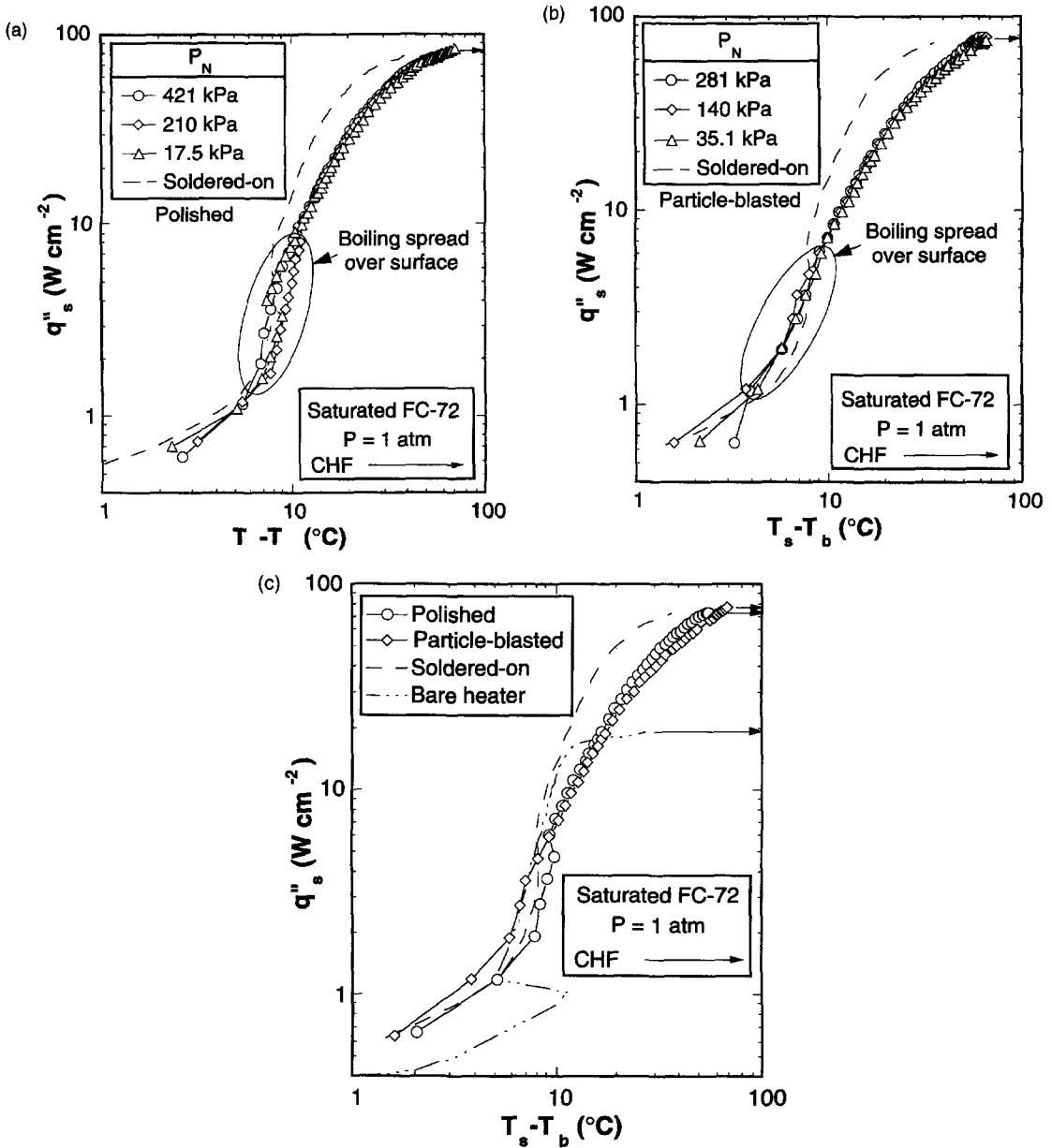


Fig. 7. Effect of contact pressure on boiling performance using pressed-on fin with: (a) polished and (b) particle-blasted contacting surfaces; (c) pressed-on fins and bare heater compared.

At 1.80 W cm^{-2} , just after incipience on both fins, boiling on the soldered-on fin occurs at only a few nucleation sites at the fin base. As the heat flux is increased, the departing bubbles from these sites become larger but the number of nucleation sites remains small. With the pressed-on fin, however, the boiling is not restricted but spreads to multiple sites around the perimeter of the interface quickly as the power is increased. The increased area of boiling coverage with the pressed-on fin at low heat fluxes translates to better convection, measured as lower heater temperatures. At higher heat fluxes, as shown in the figure, boiling on both fins occurs over nearly the same fraction of the fin area and there is little

difference between the soldered-on and pressed-on cases. The constant value of the interface resistance, shown in Fig. 9, as the heat flux is increased beyond 7 W cm^{-2} , also suggests that little is changing at the fin-heater contact and that boiling on the perimeter of the fin dominates any heat transfer from the interface region. Thus, while the interface does serve to promote earlier boiling incipience, at higher fluxes it behaves purely as a thermal contact resistance. However, in spite of this additional conduction resistance, as Fig. 7(c) shows, the boiling behavior with the fin is considerably improved over boiling from a bare surface, seen as a three-fold increase in the critical heat flux.

Average roughness data for similarly prepared, pol-

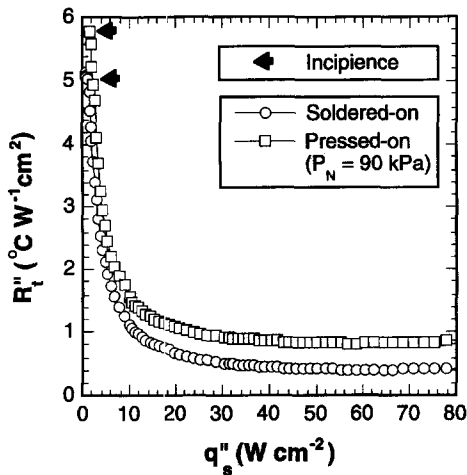


Fig. 8. Comparison of fin resistances for soldered-on and pressed-on copper fins with flat, polished contacting surfaces.

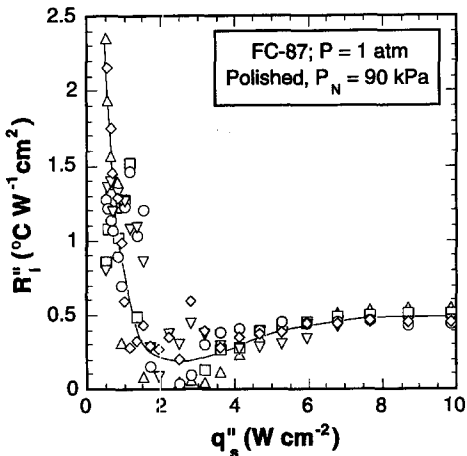


Fig. 9. Effective interface resistances for several tests.

ished surfaces are given in Bernardin and Mudawar [13] and are on the order of $0.1 \mu\text{m}$. Comparison with the thermal contact resistance model of Antonetti and Whittle [14], which was developed from published contact resistance data for a variety of surface materials with roughness on the same order as this study, shows good agreement with a thermal contact resistance value of around $0.475^\circ\text{C W}^{-1} \text{cm}^2$. However, this is only useful for approximating the contact resistance as large scale roughness, resulting from the machining process, and conduction through the interstitial fluid were not considered in the calculations.

Several tests were run to determine the amount of hysteresis in the interface resistance and boiling incipience behavior. In these tests, once boiling had occurred over the entire surface, the power was decreased manually to zero heat flux. This was done gradually, allowing the system to reach steady-state at each step. Figure 12 shows results from one of the runs. Because the interface does serve to promote early nucleation, hysteresis in the boiling behavior and

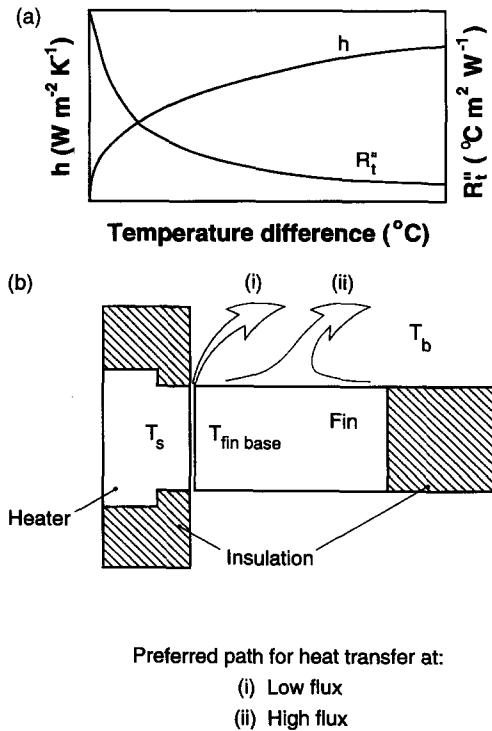


Fig. 10. (a) Natural convection on a horizontal cylinder and (b) paths of heat transfer for pressed-on fin.

interface resistance is small, as shown by the similarity in the increasing heat flux and decreasing heat flux curves.

3.3. Fluorinert penetration

Over the course of several test runs, small amounts of a nonvolatile substance built up in the interface between the pressed-on fin and heater surface. This substance was identified, through spectroanalysis, as a plasticizer known as diisooctyl phthalate, which has a saturation temperature on the order of 200°C . This substance is found in both TYGON and polyethylene tubing and was likely leached, by the Fluorinert liquid, out of the submerged polyethylene cooling coil. The amount of the plasticizer in the liquid is small enough that the boiling characteristics are not significantly affected and tests run with clean and contaminated liquid yielded similar results. The test chamber was filled with fluid after the surface extension was assembled and drained before disassembly. The build up of the substance in the very small interface region, then, suggests that the low contact angle Fluorinert liquid actually penetrated the region and boiled off, leaving the plasticizer.

4. MODELING OF CONVECTION COEFFICIENT FOR FINITE LENGTH CYLINDRICAL FIN

As the interface resistances show, the pressed-on fin offers an advantage over the soldered-on. The interface promotes earlier nucleation and boiling spread, as well as additional convection from fluid circulation.

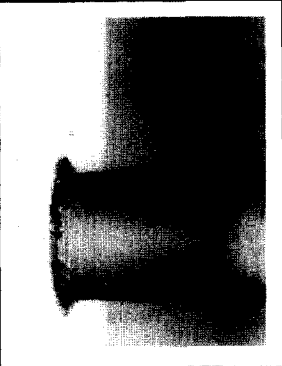
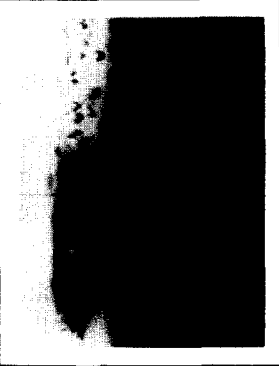
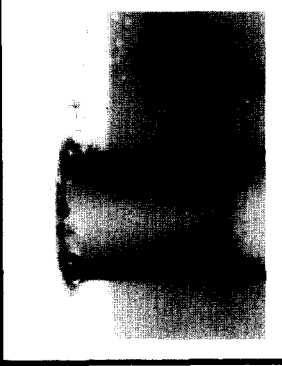
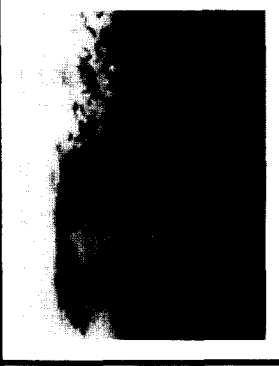


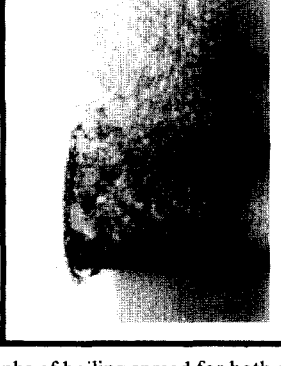
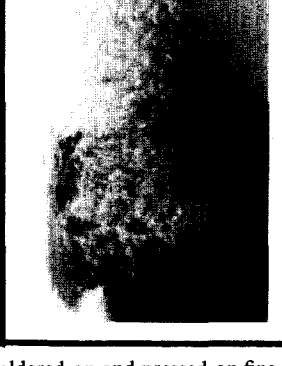
q_s'' (W cm ⁻²)	Soldered-on	Pressed-on
1.80		
2.14		
7.18		
14.26		

Fig. 11. Photographs of boiling spread for both soldered-on and pressed-on fins.

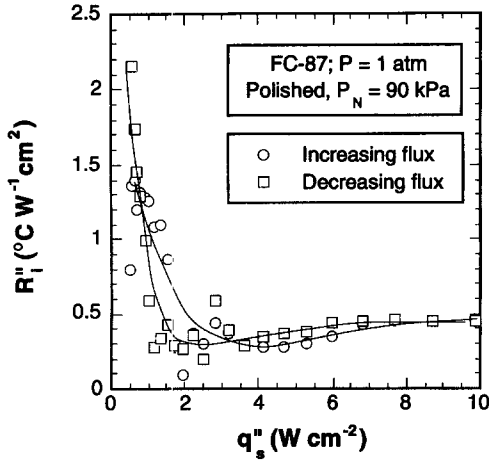


Fig. 12. Lack of hysteresis in interface resistance.

Optimization, then, of a boiling heat sink may involve some non-cylindrical fin, to maximize fin effectiveness, as well as some interface or contact geometry designed to repeatedly enhance nucleation and boiling spread. A basis for numerically modeling the heat conduction and surface convection from the fin in boiling is important for determining the interface contact resistance and heater temperatures for any interface or fin geometry. Because boiling convection coefficients are highly temperature dependent, there is no simple analytical solution for boiling on a fin as there is with a constant convection coefficient. Additionally, the fin is of finite length and is heated from one end. As a result, the fin temperature is not uniform, precluding the use of correlations for boiling on an infinitely long, isothermal cylinder.

To calculate the boiling behavior for the finite length fin, the heat diffusion equation was solved, using a finite difference code, for a range of uniform heat fluxes applied at the base of the fin. The fin tip was prescribed as adiabatic and a circumferentially averaged boiling curve, assuming an isothermal perimeter for each discrete cross-section, was used for the convection on the perimeter, simplifying the heat diffusion equation in cylindrical coordinates to:

$$\frac{1}{r} \frac{\partial}{\partial r} \left(r \frac{\partial T}{\partial r} \right) + \frac{\partial^2 T}{\partial z^2} = 0 \quad (2)$$

for steady, axisymmetric conduction. This averaging involved measurement of the boiling behavior for a bare heater at a range of positions, Fig. 13, with respect to gravity. The test heater used for the orientation data was a 12.7 mm square heater, rather than the 12.7 mm diameter circular one used in the other tests. The temperature data from the various orientations, every 15° from 0° (horizontal, upward facing) to 165°, were simply averaged to obtain a boiling curve representative of the entire perimeter and fit with a continuous arctangent function, given in Table 2. The data from the 180° degree surface (horizontal, downward-facing) were neglected because produced vapor

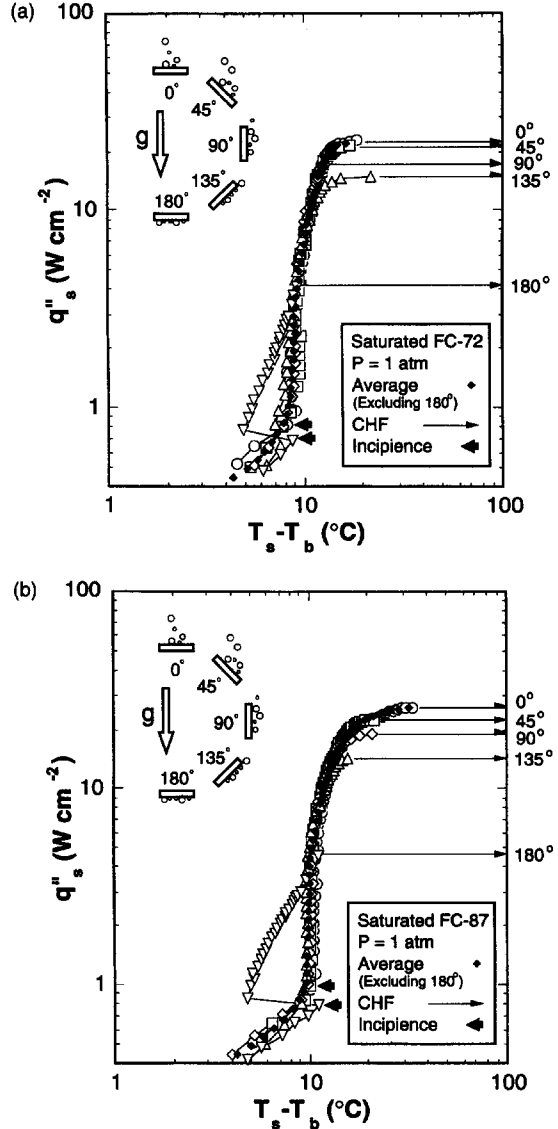


Fig. 13. Bare surface boiling curves for various angles and average boiling curves for: (a) FC-72; and (b) FC-87.

could not escape and nucleate boiling incipience was closely followed by critical heat flux. The boiling data for various heater orientations show, as has been suggested before, that nucleate boiling behavior is independent of the surface orientation with respect to gravity.

Figure 14 shows the heat flux versus fin base temperature and compares the numerical solution with the experimental results and the case of an isothermal fin. The single phase region was solved using the Churchill and Chu [12] and Morgan [15] correlations for horizontal cylinders as the convection boundary condition. The single phase region was terminated at the point where the natural convection correlations intersected the average nucleate boiling curve. The results show good approximation for heat transfer from the horizontal cylinder up to heat fluxes near CHF. The heater used for the orientation boiling behavior

Table 2. Convection boundary conditions used in numerical fin solution

Natural convection on long, isothermal, horizontal cylinder (Morgan [15] and Churchill and Chu [12])

Morgan :

$$\overline{Nu}_D = \frac{\bar{h}D}{k_f} = B_1 (Ra_D)^{m_1}$$

where :

Ra_D	B_1	m_1
10^{-10} – 10^{-2}	0.675	0.058
10^{-2} – 10^2	1.02	0.148
10^2 – 10^4	0.850	0.188
10^4 – 10^7	0.480	0.250
10^7 – 10^{12}	0.125	0.333

Churchill and Chu :

$$\overline{Nu}_D = \left\{ 0.60 + \frac{0.387 Ra_D^{1/6}}{[1 + (0.559/Pr_f)^{9/16}]^{8/27}} \right\}^2 \quad 10^{-5} < Ra_D < 10^{12}$$

Fit of average nucleate boiling curve data (present study)

FC-72 :

$$\bar{h} = \frac{9.95}{T_s - T_b} \left\{ \tan^{-1} \left[\frac{T_s - T_b - 10.80}{2.22} \right] + 1.01 \right\}$$

FC-87 :

$$\bar{h} = \frac{16.54}{T_s - T_b} \left\{ \tan^{-1} \left[\frac{T_s - T_b - 9.95}{4.36} \right] + 0.20 \right\}$$

Pool boiling CHF on long, isothermal, horizontal cylinder (Sun and Lienhard [16])

$$\frac{q''_{\max}}{q''_{\max,F}} = \frac{6}{\pi^2 \sqrt{3}} \frac{(R' + \Delta)^{3/2}}{R'} \quad R' + \Delta \leq 4.28$$

$$\frac{q''_{\max}}{q''_{\max,F}} = \frac{3^{3/4}}{\pi} \frac{(R' + \Delta)}{R'} \quad R' + \Delta > 4.28$$

where :

$$\Delta = [2.54R' + 6.48R' e^{(-3.44\sqrt{R'})^{2/3}}] - R' \quad R' < 3.47$$

$$\Delta = 0.233R' \quad R' > 3.47$$

$$R' = R \sqrt{\frac{g(\rho_f - \rho_g)}{\sigma}}$$

$$q''_{\max,F} = 0.149 \rho_g^{1/2} h_{fg} \sqrt[4]{g\sigma(\rho_f - \rho_g)} \quad \text{Lienhard et al. [17]}$$

measurements was on the order of the size of the cylinder, thereby accounting, to some extent, for the interaction between bubble production sites at higher fluxes. However, numerical solution using the averaged curve still deviates significantly at fluxes near critical, suggesting that the interaction is, in fact, more significant. The Lienhard *et al.* [16] relation for the critical heat flux, using the fin base temperature and

shown in Fig. 14 as CHF_{cor.} agrees well with the experimental data. Table 2 summarizes the relations used for surface convection in the numerical fin solution.

5. CONCLUSIONS

The goals of this study were to examine performance enhancement for boiling heat dissipation in

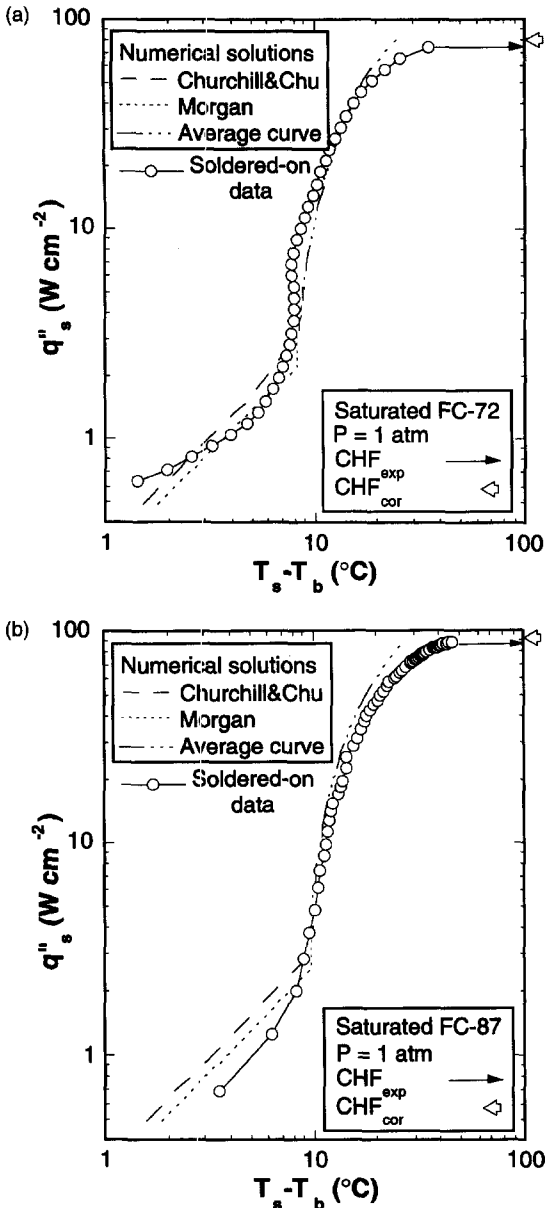


Fig. 14. Comparison of numerical fin solutions to correlations and soldered-on fin data: (a) FC-72; and (b) FC-87.

highly wetting fluids. Because possible applications include electronic component cooling, enhancement involving an extended surface held to the heat source with low forces in a non-permanent manner was considered. The important results follow :

(1) At the low mechanical contact pressures allowed on electronic components, the thermal contact resistance shows small dependence on constant pressure. However, even with contact pressures as low as 17.5 kPa with the non-optimized cylindrical fin, the maximum boiling heat dissipation is increased by a factor of three over boiling from a bare surface while maintaining low heater surface temperatures. This demonstrates the potential of non-permanent, low-

force fins combined with boiling for high performance cooling.

(2) The highly-wetting Fluorinert liquids used in these tests are capable of penetrating extremely small regions. Such regions, including the tiny crevice at the interface of the heater and the cylindrical fin, serves to restrict the fluid motion and cause it to superheat and nucleate earlier. The pressed-on fin demonstrates the advantage over the soldered-on fin that boiling begins slightly earlier, spreads more evenly, and shows little hysteresis or, deviation upon decreasing the heat flux.

(3) Nucleate boiling convection is independent of the orientation of the surface with respect to gravity. A method of approximating boiling convection for use in numerical solution of arbitrary extended surface geometry in nucleate boiling is presented. The results, combined with existing correlations for natural convection heat transfer and the critical heat flux value, closely match the actual, soldered-on fin behavior. Once the fin boiling resistance or, relationship between the heat flux and base temperature for a particular geometry, is known, it may be used to compute the actual heat flow into the fin for other areas and geometries of contact based on knowledge of the interface geometry and heat transfer behavior.

Acknowledgements—This material is based upon work supported in part by IBM Data Systems Division and a National Science Foundation Graduate Research Fellowship. The authors also appreciate receiving FC-72 and FC-87 fluid samples from the Industrial Chemical Products Division of 3M.

REFERENCES

1. Tousignant, L., 3M Company Specialty Chemicals Division, St Paul, MI, 1994, personal communication.
2. Reeber, M. D. and Friese, R. G., Heat transfer of modified silicon surfaces. *IEEE Transactions*, 1980, 3, 387–391.
3. Nakayama, W., Nakajima, T. and Hirasawa, S., Heat sink studs having enhanced boiling surfaces for cooling of microelectronic components. *ASME Paper 87-WA/HT-89*, 1984.
4. Anderson, T. M. and Mudawar, L., Optimization of enhanced surfaces for high flux chip cooling by pool boiling. *ASME Journal of Electronic Packaging*, 1993 115, 89–100.
5. Webb, R. L., The evolution of enhanced surface geometries for nucleate boiling. *Heat Transfer Engineering*, 1981, 2, 46–68.
6. Chyu, M. C. and Mghamis, A. M., Effect of cylindrical wall attachment on nucleate boiling. *ASME HTD*, 1991, 114, 69–74.
7. Hsu, Y. Y. and Graham, R. W., *Transport Processes in Boiling and Two-Phase Systems*. Hemisphere, Washington D.C., 1976.
8. Goth, G. F., Zumbrennen, M. L. and Moran, K. P., Dual-tapered piston (DTP) module cooling for IBM Enterprise System/9000 systems. *IBM Journal Research and Development*, 1992, 36, 805–816.
9. Cash, D. R., Klein, G. J. and Westwater, J. W., Approximate optimum fin design for boiling heat transfer. *ASME Journal of Heat Transfer*, 1971, 93, 19–24.
10. Eid, J. C. and Antonetti, V. W., Small scale thermal

- resistance of aluminium against silicon, *Proceedings of the Eighth Interactions Heat Transfer Conference*, San Francisco, CA, 1986, Vol. 2, pp. 659–664.
11. Jakob, M., *Heat Transfer*, Wiley, New York, 1949.
 12. Churchill, S. W. and Chu, H. H. S., Correlating equations for laminar and turbulent free convection from a horizontal cylinder. *International Journal of Heat and Mass Transfer*, 1975, **18**, 1049–1053.
 13. Bernardin, J. D. and Mudawar, I., Experimental and statistical investigation of changes in surface roughness associated with spray quenching. *International Journal of Heat and Mass Transfer*, 1996, **39**, 2023–2037.
 14. Antonetti, V. W. and Whittle, T. D., An approximate thermal contact conductance correlation. *ASME HTD*, 1991, **170**, 35–42.
 15. Morgan, V. T., The overall convective heat transfer from smooth circular cylinders. *Advances in Heat Transfer*, ed T. F. Irvine and J. P. Harnett, 1975, **11**, 199–264.
 16. Lienhard, J. H., Dhir, V. K. and Rihard, D. M., Peak pool boiling heat-flux measurements on finite horizontal flat plates. ASME Paper 73-WA/HT-30, 1973.
 17. Sun, K. H. and Lienhard, J. H., The peak boiling heat flux on horizontal cylinders. *International Journal of Heat and Mass Transfer*, 1970, **13**, 1425–1438.